A New Formulation for the Critical Temperature for Contrail Formation

RICH F. COLEMAN

The Aerospace Corporation, Silver Spring, Maryland

(Manuscript received 16 August 1995, in final form 30 May 1996)

ABSTRACT

A new formulation of the equations describing the conditions necessary for aircraft exhaust contrail formation is derived from the fundamental necessary condition. First, the original solution of Appleman is derived from the necessary condition to illustrate the continuity of the new formulation. Then the new formulation offers an analytic solution for the critical temperature T_c expressed in terms of water vapor mixing ratio and atmospheric pressure, rather than in terms of relative humidity and pressure, thus avoiding potential forecast errors associated with the temperature sensitivity inherent in relative humidity. A variety of results is presented, including a comparison with the seminal results of Appleman, a comparison of the sensitivity of T_c to perturbations in relative humidity versus perturbations in mixing ratio, and some typical results for actual atmospheric conditions. The clear superiority of a formulation based on mixing ratio rather than relative humidity is seen in the reduced sensitivity of T_c to errors or uncertainties in the input atmospheric variables.

1. Introduction

Contrail formation has been a subject of interest in atmospheric physics and to high-altitude aircraft pilots since World War II, when a new generation of high-altitude bombers began producing contrails routinely. Contrail forecasting remains a subject of considerable interest to military weather forecasters and pilots since contrails unequivocally indicate the presence of aircraft. Since the presence of contrails can significantly increase the probability that an aircraft will be detected, either by ground-based observers or by other aircraft, mission planners adjust routes and flight levels based on contrail forecasts in an attempt to minimize the chance of detection. As recently as 1989 (cf. Peters 1993), the Deputy Chief of Staff, Operations, for Strategic Air Command (SAC) expressed concern over the accuracy of the contrail forecasts provided to SAC aircrews by Air Weather Service (AWS). This concern has resulted in new activity in contrail forecasting research and has offered an opportunity to revisit the original analysis of the problem.

Considerable research on the subject of contrails produced by propeller-driven aircraft was done in the 1940s, as cited by Appleman (1953). The fundamental paper on the formation of contrails by jet aircraft (A/C) was published by Appleman (1953). In that paper Appleman described the thermodynamics of contrail formation and provided a method of forecasting the occurrence of contrails based on forecasts of relative humidity and pressure. Appleman's forecasting method rests on four assumptions associated with contrail phenomena and with his analysis of their formation:

(i) contrails are composed of ice crystals;
(ii) ice crystals do not nucleate directly from the vapor state, so contrails cannot form unless the A/C wake reaches saturation with respect to water;
(iii) from combustion of A/C fuel the ratio of the amount of water injected into the wake to the amount of heat injected into the wake is a constant for all jet A/C (this ratio is called the contrail factor);
(iv) for a given ambient relative humidity and pressure, there is a critical temperature below which contrails will always form (but not necessarily persist) in A/C wakes.

Appleman also supplied a criterion for the water content needed for contrails to persist and remain visible, and several researchers have addressed that subsequently. However, this paper is concerned only with contrail onset since saturation with respect to water ensures enough water is available to form a visible ice crystal contrail, even if it sublimes shortly thereafter. Subsequent to Appleman's original paper, Air Weather Service and others conducted and/or funded studies intended to validate the forecasting method, to identify potential sources of error in the method, and to develop alternate forecasting methods.

Appleman continued to work on contrails under Project CLOUD TRAIL, which found discrepancies between observed and predicted contrail formation conditions. He examined the effects of A/C engine set-

Corresponding author address: Rich F. Coleman, Sr. Project Engineer, NPOESS Integrated Program Office, The Aerospace Corporation, 8455 Colesville Road, Suite 1450, Silver Spring, MD 20910.
E-mail: rcoleman@ipo.noaa.gov

ting, that is, assumption (iii), on contrail formation (Appleman 1954). In an AWS report in 1957, Appleman consolidated work from both previous papers, plus additional work from CLOUD TRAIL, and provided the basis for the AWS standard forecasting manual still in use today (cf. AWS 1981). In that report, Appleman also developed an empirical forecasting method based on the frequency of occurrence of contrails reported by pilots (PIREPS), which he provided as an adjunct to his main forecasting method, modified his original conclusions as to the amount of ambient water necessary to allow contrails to persist and be seen, and provided representative values of relative humidity (RH) to be used by forecasters when no reliable forecast RH value was available. An interesting observational result was that horizontal temperature gradients at or near the tropopause could average as high as 0.099°C km^{-1}.

Assumptions (i) and (ii) have been examined repeatedly. Pilie and Jiusto (1958) examined contrails formed in a laboratory cloud chamber and found evidence of liquid particles in some contrails at $T < -40$°C, but that finding has not been replicated. Murcray (1970) studied contrails at ground level in interior Alaska winter at temperatures less than or equal to −40°C, mostly from Boeing 727 A/C. He found the liquid phase always occurred first, followed within 1 s by freezing. He found no occurrence of long-term liquid phase contrail particles. Initial contrails showed spherical ice particles with a mode diameter of order 2 μm and with at least 80% having a diameter 4 μm or smaller. Knollenberg (1972) made flight test observations of contrails that appeared to occur below water saturation; however, it is not clear if the meteorological conditions presented were measured in situ or were taken from the closest recent sounding. Also, the A/C was operated at an artificially low airspeed due to flaps being set to partial approach; this was to aid particle collection efforts. However, the unusual engine setting almost certainly altered the contrail factor (cf. Saatzer 1995), which also could explain Knollenberg's observation. Knollenberg's particle counts tend to confirm Murcray's finding that all liquid particles freeze rapidly rather than persisting to be scavenged by ice particles. Sassen (1979) photographed iridescence in an A/C contrail, a phenomenon typically assumed to confirm the presence of water droplets. However, iridescence is associated with diffraction from small spherical particles, and Murcray's results show that ice particles of that type are present in initial contrails. Interestingly, Sassen's results require particles with diameters of 1–3 μm, corresponding almost exactly with Murcray's observations. At present there remains no compelling evidence that either assumption (i) or (ii) is invalid.

TABLE 1. Values of the contrail factor C_F for several engine types.

Engine type	C_F
Nonbypass	0.036
Low bypass	0.040
High bypass	0.049
Original Appleman	0.0336

TABLE 2. Values for constants for saturation vapor pressure expression.

$a_1 = 54.8758$
$a_2 = 58.0691$
$a_3 = 6790.51$
$a_4 = 1.44078 \times 10^{-18}$
$a_5 = 5.02808$
$b_1 = 2999.992$
$b_2 = 0.069998$

Several scientists have addressed assumption (iii). Appleman (1954) found no change in contrail factor with engine setting, altitude, or airspeed. Scorer and Davenport (1970) noted, however, that fuels with different proportions of hydrogen than kerosene (JP-4) would yield greater or lesser amounts of water for essentially the same amount of heat, thus violating assumption (iii). Work by Peters (1993) and Saatzer (1995) has shown conclusively that different engine types, as determined by the amount of ambient air injected into the exhaust, give rise to different contrail factors, requiring contrail factor to be treated as an independent variable in contrail formation. Saatzer additionally showed that engine setting has a significant effect on contrail factor.

A number of scientists subsequent to Appleman have addressed the problem of determining the critical temperature and forecasting the onset of contrails. Pilie and Jiusto (1958) presented a major simplification of Appleman's approach to finding the critical temperature, discussed further in section 2. Scorer and Davenport (1970) extended the approach of Pilie and Jiusto to include some alternate fuel types. All of these approaches, including Appleman's original formulation, yield a solution graphically. Appleman (1957), Miller (1990), Bjornson (1992), and Peters (1993) have presented empirically based solutions for the critical temperature. However, the standard forecasting method still in use, as documented in AWS (1981) and used in validation studies by Miller (1990), Bjornson (1992), and Peters (1993), is the Appleman method, modified to allow different values of the contrail factor. This present paper offers a new formulation of the equation for the critical temperature for contrail formation in terms of a variable contrail factor, mixing ratio, and pressure rather than RH, pressure, and a constant contrail factor. In addition, the new formulation is an analytic solution for critical temperature and thus will offer an easier implementation for computational forecasting than previous graphical solution methods. The new formulation also will result in increased fore-

cast accuracy since errors in RH depend on both errors in ambient temperature and in mixing ratio.

Rather than derive the new formulation in the traditional way based on the thermodynamics of jet aircraft exhaust, a fundamental necessary condition for contrail formation is presented and then shown to lead to the Appleman curves. The new formulation for critical temperature is then derived from the fundamental condition, followed by a determination of the sensitivity of the two formulations to small perturbations in the independent variables. Finally, the inherent accuracy of the two formulations is discussed in light of current forecasting methods, followed by some representative results.

2. Fundamental condition for contrail formation

The fundamental condition for contrail formation may be stated as follows. If the water vapor mixing ratio w_p at some point in the A/C wake equals or exceeds the saturation mixing ratio w_s at the temperature T_p anywhere in the exhaust plume, then a contrail can occur:

$$w_p \geq w_s \quad \text{at} \quad T_p, \tag{1}$$

where, of course, the conditions w_p and T_p occur at point p in the wake. This equation, if the mixing ratio and coincident temperature are available, is the easiest approach to determining the critical temperature T_c, that is, the ambient temperature for which Eq. (1) becomes an equality.

This condition was noted by Appleman (1953) but used only to determine the amount of water required beyond the ambient RH values necessary to maintain saturation in the wake in the presence of the added heat from combustion. Pilie and Jiusto (1958) made use of it and the contrail factor to greatly simplify Appleman's graphical method of determining T_c. They made use of the fact that the ratio of water added to the wake to the heat added to the wake (the contrail factor) can be represented by a line with slope equal to its value on a phase diagram of mixing ratio versus temperature. If the saturation mixing ratio is plotted on the same diagram, then the tangent point of the two curves is T_c, that is, the temperature above which saturation in the wake cannot occur. They used this method to determine T_c for a variety of pressures and RH values and for vapor pressure values, producing modified forecast tables.

However, it is possible to go further using this condition: it is possible to derive nongraphical expressions for T_c. A transcendental expression that replicates the original Appleman results may be derived, and further, an analytic expression for T_c may be derived that avoids the use of RH entirely. This latter expression has a variety of positive consequences, as will be shown in subsequent sections.

3. Appleman curves derived from fundamental condition

Appleman's original curves are derived from Eq. (1) by first subtracting the ambient mixing ratio w_a from

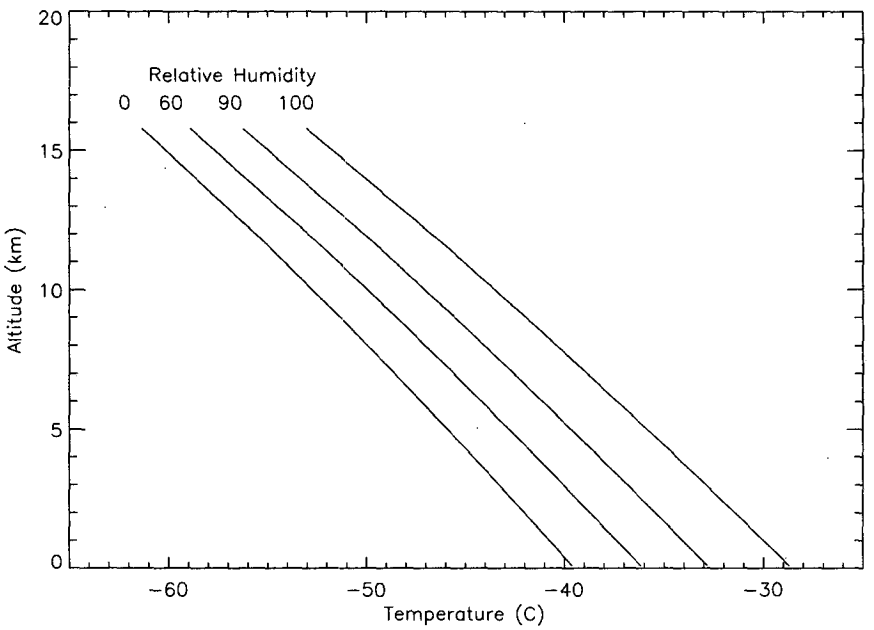

FIG. 1. Replicating Appleman's critical temperatures for contrail formation at various relative humidities and altitudes.

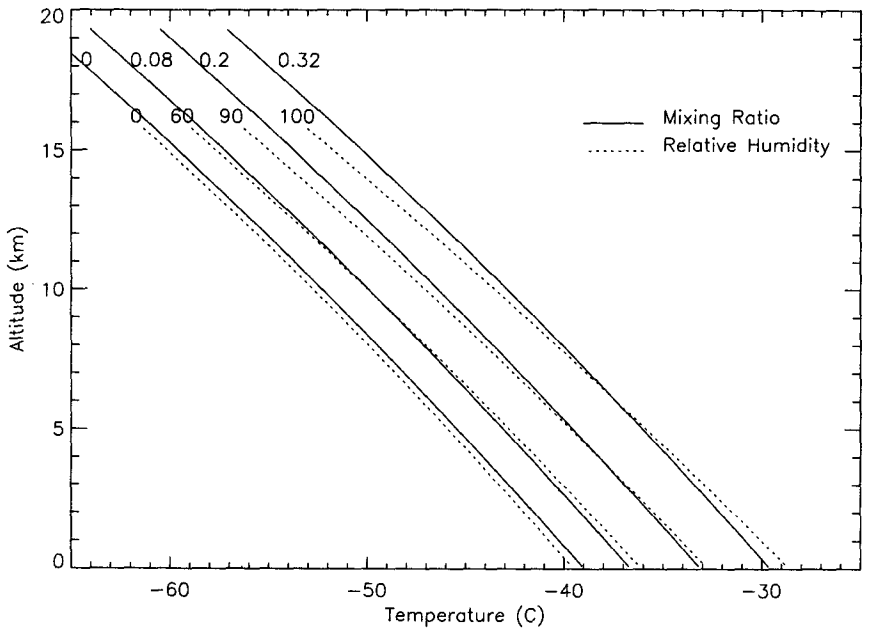

FIG. 2. Comparison of T_c for formulations based on mixing ratio and on relative humidity.

both sides, then dividing both sides by the difference between the temperature of the entrained air in the wake at point $p(T_p)$ and the ambient temperature T_a. Then the inequality becomes

$$\frac{w_p - w_a}{T_p - T_a} \geqslant \frac{w_s(T_p) - w_a}{T_p - T_a}. \tag{2}$$

The left-hand side is now the ratio of the change in water vapor mixing ratio to the change in temperature due to exhaust. These quantities are defined as follows in Appleman's original paper (1953).

The change in the water vapor mixing ratio of an air parcel, resulting from the combustion of a unit mass of fuel in an A/C jet engine, which mixes with an ambient parcel of mass N, may be written as (following Appleman)

$$\Delta w = w_p - w_a = 1000 \frac{m_w}{m_e N} \text{ (g kg}^{-1}\text{)}, \tag{3}$$

where w_p is the water vapor mixing ratio at point p in the plume, w_a is the ambient water vapor mixing ratio, N is the mass of ambient air parcel that mixes with unit mass of exhaust, m_w is the mass of water vapor in A/C exhaust, and m_e is the mass of exhaust parcel. Note that Appleman (1953) gives $\Delta w = 1000(1.4/12N)$ for all fuels and engines.

The change in temperature due to the energy released in the A/C exhaust by combustion of a unit mass of fuel (again following Appleman) is given as

$$\Delta T = T_p - T_a = \frac{E}{m_e c_p N}, \tag{4}$$

where E is the energy released, c_p is the specific heat of air at constant pressure, T_p is the temperature of the mixed air parcel at point p, and T_a is the ambient temperature. Note that Appleman (1953) gives $\Delta T = 10^4(0.24 \times 12N)^{-1}$ for all fuels and engines.

The ratio of these two quantities was assumed by Appleman to be a constant based on early work on jet engines. This quantity has come to be called the contrail factor C_F and, while not a constant, still has only a limited range of values. Unfortunately the individual values for the increase in the mixing ratio and the temperature are typically not available for jet engines; instead this ratio is the only available quantity. The ratio itself is

$$C_F = \frac{\Delta w}{\Delta T} = 1000 \frac{m_w c_p}{E}. \tag{5}$$

Thus the left side of Eq. (2) is just Appleman's contrail factor. A set of values for C_F at 35 000 ft, grouped by engine type, is given by Peters (1993) and is shown in Table 1.

To address the right side of Eq. (2), it is noted that the water vapor mixing ratio for a saturated parcel w_s is a function of the temperature and pressure of the parcel. The definition of mixing ratio and the equations of state for dry air and water vapor give

$$w_s = 1000 \frac{e_s}{p - e_s} \frac{M_v}{M_a} \approx 1000 \frac{e_s}{p} \frac{M_v}{M_a}, \tag{6}$$

where p is pressure, e_s is saturation vapor pressure, M_a is molecular weight of dry air, and M_v is molecular weight of vapor. The final approximation is appropriate

since for temperatures T below freezing, $p \gg e_s$. The saturation mixing ratio and the ambient mixing ratio are related through the relative humidity as follows:

$$w_a = w_s \frac{\mathrm{RH}}{100}, \tag{7}$$

where RH is relative humidity.

The saturation vapor pressure is given by [after Goff–Gratch as shown in List (1968) with some manipulation]

$$\ln(e_s) = 54.8758 + 58.0691 e^{-2999.992/T} - \frac{6790.51}{T} + 1.44078 \times 10^{-18} e^{0.069998T} + 5.02808 \ln(T). \tag{8}$$

This may be rewritten as follows:

$$e_s = \exp\left[a_1 + a_2 e^{-b_1/T} - \frac{a_3}{T} + a_4 e^{b_2 T} + a_5 \ln(T) \right], \tag{9}$$

where the values for the constants are given in Table 2.

Returning to the fundamental condition, as expressed in Eq. (2), the inequality may now be rewritten as follows, after substituting Eq. (7) for RH:

$$C_F \geqslant \frac{100 w_s(T_p) - w_s(T_a)\mathrm{RH}}{100 \Delta T}. \tag{10}$$

The critical temperature T_c is defined as the ambient temperature T_a at which Eq. (10) becomes an equality:

$$100 \Delta T C_F - 100 w_s(T_c + \Delta T) + w_s(T_c)\mathrm{RH} = 0, \tag{11}$$

noting that $T_p = T_a + \Delta T$.

Substituting the value for the ratio of the vapor and air molecular weights, 0.621979, gives

$$100 p \Delta T C_F - 62197.9 e_s(T_c + \Delta T) + 621.979 e_s(T_c)\mathrm{RH} = 0. \tag{12}$$

As a final step, substituting Eq. (9) into Eq. (12) gives

$$K_1 p \Delta T C_F - K_1 K_2 \exp\left[a_1 + a_2 e^{-b_1/(T_c+\Delta T)} - \frac{a_3}{T_c + \Delta T} + a_4 e^{b_2(T_c+\Delta T)} + a_5 \ln(T_c + \Delta T) \right] + \mathrm{RH} K_2 \exp\left[a_1 + a_2 e^{-b_1/T_c} - \frac{a_3}{T_c} + a_4 e^{b_2 T_c} + a_5 \ln(T_c) \right] = 0, \tag{13}$$

where $K_1 = 100$, $K_2 = 621.979$, and the constants a and b have been given in Table 2.

In Eq. (13) the pressure, relative humidity, and temperature dependence may be seen directly. The impact of the extent to which the A/C exhaust parcel mixes with the ambient air also may be seen directly since ΔT is inversely proportional to this mixing. This equation, being transcendental in T_c, has no analytic solution. Previous methods for forecasting contrail formation, implicitly based on this equation, have used graphical approaches to obtaining a solution. They also have ignored the effects of ΔT by taking the highest T_c at which a contrail can form and assuming that at some point in the contrail the mixing ratio associated with that particular ΔT will occur. Equation (13) is equivalent to Appleman's original result, which can be shown by comparing results from Eq. (13) with his numerical results.

To replicate the data from Appleman's (1953) Fig. 4, T_c was computed at the same pressure levels and relative humidity values using the ΔT value that gives the highest critical temperature at each pressure level. The resulting data are shown in Fig. 1, where the zeros of Eq. (13) were determined numerically rather than using graphical methods. The data are plotted as a function of altitude rather than pressure. Comparison of the values from this approach with the original Appleman tables shows the maximum difference to be less than 0.4°C across all values of RH and p.

4. New expression for critical temperature

The equation for the critical temperature may be rewritten to remove the relative humidity by using the fundamental condition given in Eq. (1). As before, the first step is to derive Eq. (2). As noted before, the left-hand side of Eq. (2) is just the contrail factor, and after substitution the equation becomes

$$C_F \geqslant \frac{w_s(T_p) - w_a}{T_p - T_a}. \tag{14}$$

This may be rewritten as an equality in terms of ΔT [as defined in Eq. (4)] and T_c as

$$\Delta TC_F - w_s(T_c + \Delta T) + w_a = 0. \quad (15)$$

Substitution of Eq. (6) for w_s into Eq. (15) gives

$$\Delta TC_F + w_a - 1000\,\frac{e_s(T_c + \Delta T)}{p}\,\frac{M_v}{M_a} = 0. \quad (16)$$

At this point, the equation may be treated as before by using the Goff–Gratch expression for saturation vapor pressure. However, unlike the case of the relative humidity formulation, here the use of Tetens's expression (Bolton 1980) for vapor pressure allows an analytic solution to be obtained. Tetens's expression is

$$e_s(T) = 6.1078 \exp\left(17.26939\,\frac{T - 273.15}{T - 273.15 + 237.3}\right). \quad (17)$$

Substituting into Eq. (16) gives

$$\Delta TC_F + w_a - \frac{621.979}{p}\,6.1078 \times \exp\left(17.26939\,\frac{T_c + \Delta T - 273.15}{T_c + \Delta T - 273.15 + 237.3}\right) = 0. \quad (18)$$

Equation (18) may be solved for T_c to give

$$T_c = 273.15 - \Delta T - 237.3 \ln\left[\frac{p(\Delta TC_F + w_a)}{6.1078K_2}\right]\left\{\ln\left[\frac{p(\Delta TC_F + w_a)}{6.1078K_2}\right] - 17.26939\right\}^{-1}. \quad (19)$$

Equation (19) is a fundamental equation for critical temperature and represents an alternate formulation to the original Appleman result. The two are compared below.

Figure 2 shows a comparison of the two formulations for critical temperature for the case of a low-bypass engine ($C_F = 0.034$) and an exhaust mixing resulting in a temperature difference of 9°C ($\Delta T = 9$°C). Note that the zero lines are parallel to each other but not exactly equal. This is due to the use of two different expressions for vapor pressure (Goff–Gratch versus Tetens). For situations where water is present (i.e., $w_a \neq 0$) in the ambient atmosphere, lines of constant mixing ratio do not run parallel to lines of constant relative humidity, as is to be expected. Note that as in the case of Fig. 1, the data are plotted as a function of altitude, but the calculations are made for specific values of pressure rather than altitude. The conversion to altitude is made based on the standard approximation to the hypsometric equation

$$-\frac{2g(h_2 - h_1)}{R(T_2 + T_1)} = \ln\left(\frac{p_2}{p_1}\right), \quad (20)$$

where g is the acceleration of gravity, R is the ideal gas constant, and h_i is the height of ith point.

5. Effects of differences in exhaust mixing

As an exhaust parcel moves downstream from the engine nozzle it mixes with the ambient atmosphere and as a result it cools and dries. This is a competing pair of processes in terms of creating a condition of supersaturation, and this is seen in the behavior of the critical temperature as a function of mixing. The parameter that indicates the extent of mixing is the temperature difference between the ambient air and the parcel, ΔT. When the parcel leaves the nozzle, the value of ΔT is large, and the parcel has not mixed much with the surrounding air. As it moves downstream, ΔT decreases as the parcel mixes with the ambient air.

The plot in Fig. 3 shows the effects of mixing on the critical temperature in the cases where the ambient water vapor mixing ratio is zero, where it is 0.12 g kg^{-1}, and where it is 0.42 g kg^{-1} at 300 mb (about 9-km altitude) and $C_F = 0.04$ (low-bypass). Similar behavior is observed at other pressure levels and contrail factors.

As can be seen, as the value of ΔT changes, the critical temperature passes through a maximum for each water vapor mixing ratio except for the one that corresponds to saturation (RH = 100), which in this case is 0.42 g kg^{-1}. It is also apparent that the ΔT that gives a maximum in T_c changes with mixing ratio, but not very much, and that the value of ΔT where the maximum is reached decreases with increasing w_a. Because exhaust parcels pass through all of the values of ΔT in each plume this cannot really be described as a sensitivity; it is appropriate to select the maximum value of T_c since the contrail need only form at one point in the exhaust.

Unfortunately, the derivative of Eq. (19) with respect to ΔT gives an equation with no analytic solution, so determining the ΔT for which T_c is a maximum must be done numerically. However, numerical analysis re-

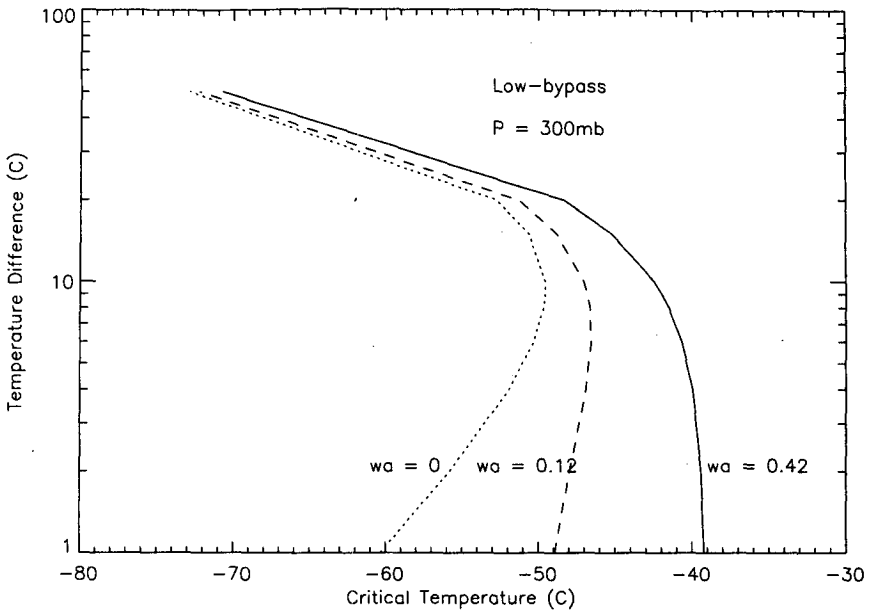

FIG. 3. Critical temperature at several mixing ratios as a function of temperature difference.

veals that if the derivative is set equal to zero and then solved for ΔT, that is,

$$\Delta T \text{ for which } \frac{\partial T_c}{\partial \Delta T} = 0 (\equiv \Delta T_m), \tag{21}$$

then ΔT_m may be fit with an equation of the form

$$\Delta T_m = a w_a + b \ln(p) + c, \tag{22}$$

where the values of the coefficients a, b, and c, for several values of C_F, are given in Table 3. Note that this fit allows ΔT_m to become negative for larger values of w_a, even though the actual solutions (zeros) of Eq. (21) do not. Thus to use Eq. (22), it is necessary to set it to zero at the points where it goes negative when making calculations. Term ΔT_m is explicitly included in Eq. (19) as follows:

$$T_c = 273.15 - \Delta T_m - 237.3 \ln\left[\frac{p(\Delta T_m C_F + w_a)}{6.1078 K_2}\right]\left\{\ln\left[\frac{p(\Delta T_m C_F + w_a)}{6.1078 K_2}\right] - 17.26939\right\}^{-1}. \tag{23}$$

All of the calculations in this paper for critical temperature use this equation, suitably restricted to nonnegative values.

6. Effects of differences in contrail factor

The effects of the contrail factor on the critical temperature are shown in Fig. 4. In the figure, critical temperature is shown for three values of C_F at each of three mixing ratios. There are two effects of interest as shown here. First, at any given mixing ratio, the higher the contrail factor the higher the critical temperature. This indicates that the lower the contrail factor, the higher the altitude at which contrails will form for a given mixing ratio. Since higher-bypass engines have higher contrail factors, they will form contrails at lower altitudes than lower-bypass engines.

The second effect to note is that as the mixing ratio increases, the effect of the contrail factor decreases. When there is no water available in the ambient atmosphere, the difference between low- and high-contrail-factor engines can be 3.5°C, whereas at a mixing ratio of 0.24 g kg^{-1} the difference between low- and high-contrail-factor engines is only about 2°C. In other words, as the amount of water available in the atmosphere increases, there is a decline in the effect of differences in the amount of water provided by the combustion process.

7. Sensitivity of critical temperature to perturbations in mixing ratio and relative humidity

The effects of small perturbations in the amount of moisture, as represented by the mixing ratio and by

TABLE 3. Values of the coefficients for ΔT for three values of contrail factor C_F.

	$C_F = 0.03$	$C_F = 0.034$	$C_F = 0.039$
a	−33.3333	−29.4118	−25.641
b	0.940286	0.959569	0.981363
c	3.92056	3.93463	3.94932

the relative humidity, are of interest in that they are representative of the sensitivity of the resulting critical temperature to errors or uncertainties (e.g., in forecasts) in the input value. It is of interest for each representation individually and as a comparison of the two representations. To examine these effects for relative humidity requires the use of the polynomial fit to the numerical solution to Eq. (13) for T_c. The fit was used to make comparisons with the original Appleman curves. This fit is of the form

$$T_c = \alpha + \sum_{i=1}^{4} \beta_i p^i + \sum_{j=1}^{5} \gamma_j \mathrm{RH}^j + \eta p \mathrm{RH}. \quad (24)$$

The sensitivity to RH may be seen by taking the partial derivative of Eq. (24) with respect to RH and multiplying by a small change in relative humidity. This in turn gives a corresponding change in the critical temperature. The partial of Eq. (24) is

$$\frac{\partial T_c}{\partial \mathrm{RH}} = \sum_{j=1}^{5} j\gamma_j \mathrm{RH}^{j-1} + \eta p. \quad (25)$$

The result of applying a 10% perturbation in RH is shown in Fig. 5. The result in Fig. 5 is for pressure of 1000 mb. Inspection of Eq. (22) and Eq. (24) shows that higher pressure will give a greater perturbation in T_c due to the fact that the atmosphere can contain more water vapor. Thus the result shown in Fig. 5 for 1000 mb is the maximum effect. As can be seen from the figure, the sensitivity of T_c to perturbations in RH is quite small until RH values exceed 80%. At high RH, the effect is severe, with errors of several degrees possible for RH > 90%. These perturbations are representative of the errors and uncertainties to be expected at high values of RH, where accurate measurements and forecasts are both are difficult to achieve.

The same technique may be applied to perturbations in w_a by taking the partial of Eq. (23) with respect to w_a and multiplying by a small change in mixing ratio. This in turn gives a corresponding change in the critical temperature. The partial derivative is given by

$$\frac{\partial T_c}{\partial w_a} = 237.3 \times 17.26939 \left\langle (C_F \Delta T_m + w_a) \left\{ \ln\left[\frac{p(C_F \Delta T_m + w_a)}{6.1078 K_2} \right] - 17.26939 \right\}^2 \right\rangle^{-1}. \quad (26)$$

The results of applying a 10% perturbation in w_a to Eq. (26) are shown in Fig. 6. This figure shows several interesting points. First, note that, as for the perturbation applied to RH, the 10% perturbation is representative of errors in mixing ratio. Thus, the perturbations shown in Fig. 5, which are less than 1.1°C, are representative for the altitudes of interest for the contrail forecasting problem, that is, from about 5-km altitude and up. For comparative purposes recall that for relative humidity above 80% the effect of a 10% perturbation in RH ranges from 1.25°C at 80% to 5°C at 95%. As can be seen in Fig. 6, the effect of errors in w_a on T_c is small and even at high values of mixing ratio the change in T_c is only slightly more than 1°C. As a result, as anticipated, the conversion from a formulation for T_c with a relative humidity dependence to a mixing ratio dependence significantly reduces the effect of errors in w_a. Use of this formulation should significantly reduce the effect of forecast errors in atmospheric water vapor on forecasts of T_c.

A second point of interest is the linear behavior of the perturbations in mixing ratio. This results from the fact that at ΔT_m, where the effects of w_a are actually greatest, the partial of T_c given in Eq. (26) turns out to be a constant (29.5 ± 0.2, depending on C_F). As a result, regardless of altitude (i.e., p) the effect of w_a perturbations is the same, and the smaller the mixing ratio the smaller the sensitivity. Another interesting point is that the sensitivity to mixing ratio decreases with increased C_F, although not greatly. Finally, note that at high values of w_a, the curve flattens. This is a result of reaching the limit of physically realizable values of ΔT_m (i.e., ≥ 0). The limit corresponds to reaching saturation for the pressure and temperature.

8. Sensitivity of critical temperature to perturbations in pressure

As in the case of w_a, the effects of small perturbations in atmospheric pressure are of interest in

that they are representative of errors or uncertainties (e.g., in forecasts) in the actual value for the pressure at a given altitude. These effects may be examined by taking the partial derivative of Eq. (23) with respect to p and multiplying by a small change in p. This gives a corresponding change in the critical temperature. The partial derivative is given by

$$\frac{\partial T_c}{\partial p} = 237.3 \times 17.26939 \left\langle p \left\{ \ln \left[\frac{p(C_F \Delta T_m + w_a)}{6.1078 K_2} \right] - 17.26939 \right\}^2 \right\rangle^{-1}. \quad (27)$$

The results of applying a perturbation in p equal to a 1-km change in height to Eq. (27) are shown in Fig. 7.

Figure 7 shows results for a $C_F = 0.4$. Inspection of Eq. (27) indicates that variations due to different C_F are minor since it is within a logarithm. As a result, only the low-bypass case has been plotted as it provides an intermediate value. As can be seen in the figure, T_c is more sensitive to perturbations in p than to w_a. A 1-km perturbation causes approximately a factor of 2 greater change in T_c than a 10% change in w_a except at very high values of mixing ratio. Also of note is the large variation with w_a, coupled with the fact that the lower the ambient mixing ratio, the greater the effect of perturbations in the pressure. This is of interest both in terms of forecast errors in pressure and in terms of variations in the pressure altitude measured in an aircraft versus the actual pressure at the aircraft altitude.

9. Implications for forecasting

As currently practiced by the Air Force Air Weather Service, contrail forecasting attempts to predict three things: (i) the occurrence of a contrail, (ii) the persistence of a contrail, and (iii) whether to ascend or descend if a contrail does occur at a particular altitude. Two types of forecast products are available, both based on Appleman's work (1957) as described in the AWS contrail forecast manual (AWS 1981). The first is a global product generated at Air Force Global Weather Central (AFGWC). The global product uses current analysis data for tropopause height, p, and T, for levels at 500, 400, 300, 250, 200, 150, 100, 50, and 30 mb as the initial state. This state is persisted for $p > 100$ mb out through 72 h ahead. For each forecast time in that interval (e.g., 6 h, 12 h, etc.) the forecast lapse rate is compared to the critical lapse rate from Appleman's curves, assuming 70% RH for ±300 m of the tropopause height, 40% RH below this altitude, and 10% above it. This comparison starts at 500 mb and moves upward until T falls below T_c, which is the bottom of the lowest layer. This search continues upward until T rises above T_c, which is the top of the first layer. Subsequent layers are identified in the same way. Layers less than 600 m deep are discarded, and layers less than 400 m apart are consolidated. The two deepest layers are retained for the global forecast product.

The second type of forecast is generated by AWS forecasters in the field for specific flight operations. They may use the global product or may use the Appleman curves together with a local forecast of RH, or usually a combination of both, to generate a tailored forecast. Recently, Peters (1993) has released new Appleman tables that take the known variations in C_F into account, that is, there are tables for each standard engine type except the superbypass (ducted fan) engine, as described in Table 1. These new tables are being used in the field but have yet to be implemented in the global long-term product from AFGWC.

Note that long-range and/or long-term mission planning is based on the global forecast product, and in this application it has proven to be insufficiently accurate (Peters 1993). Clearly, a number of improvements in implementation at GWC are possible, for example, using an actual forecast of RH instead of the assumed constant values noted above. However, the fundamental sensitivity to errors in forecast RH will remain, as shown by recent validation studies (Miller 1990; Bjornson 1992; Peters 1993). The formulation presented in this paper overcomes this sensitivity, and at the same time makes use of the water-mass variable (w_a) actually used in current forecast models, as well as output by satellite-sounding retrievals. In fact, in forecast applications Eq. (23) is inherently more accurate than is Eq. (13).

When used as a diagnostic equation, that is, when all the independent variables needed to compute the critical temperature are known accurately, Eq. (23) will give the same answer as Eq. (13). However, when used as a forecasting equation, it is more accurate to use the formulation based on mixing ratio (w_a). This is most easily seen by comparing the two formulations in their fundamental form before explicitly solving for T_c. The formulation, using RH given previously as Eq. (11) in the paper, is

$$100\Delta T C_F - 100 w_s(T_c + \Delta T) + w_s(T_c)\mathrm{RH} = 0, \quad (28)$$

while the formulation using w_a, given previously as Eq. (15), is

$$\Delta T C_F - w_s(T_c + \Delta T) + w_a = 0. \quad (29)$$

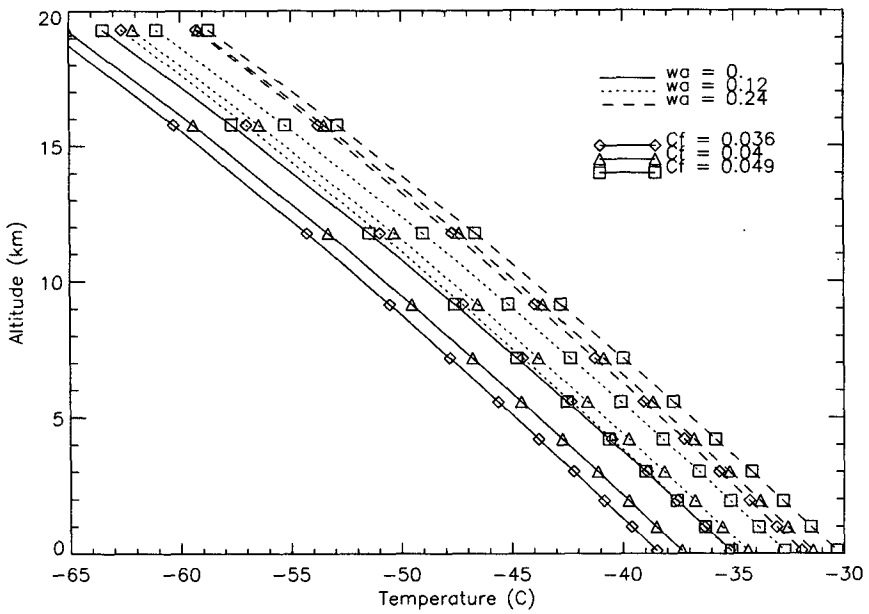

FIG. 4. Effects of different values of the contrail factor at different mixing ratios.

As can be seen, the first two terms of Eq. (28) are identical to the first two terms in Eq. (29) except for the constant multiplier, and thus show the same behavior for errors in forecasts of the input values. However, in Eq. (28), the RH in the third term depends on temperature as well as atmospheric moisture content and, thus, is susceptible to errors in temperature. In Eq. (29), the third term depends only on moisture content. Thus unless a temperature forecast is perfect (no error), the w_a formulation must give a more accurate prediction since all other variables are common to both formulations.

As an example of applying the new equation for T_c, three examples are included here. Figure 8 shows the critical temperature for an arctic atmospheric temperature and mixing ratio RAOB profile. The site was at 67.7°S, 62.88°E. Several interesting features are evident in the figure. First note that the atmosphere is quite

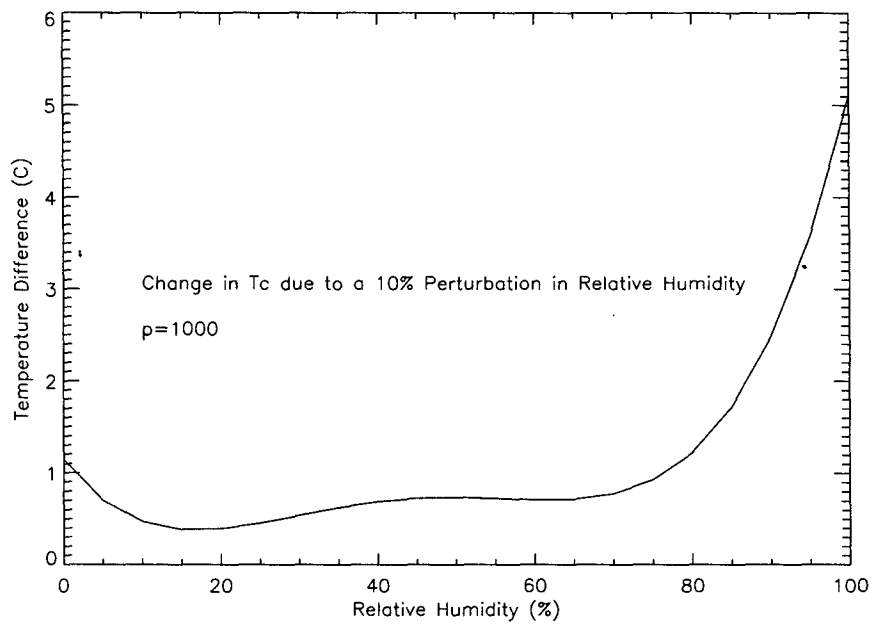

FIG. 5. Sensitivity of T_c to perturbations in RH for a nonbypass engine.

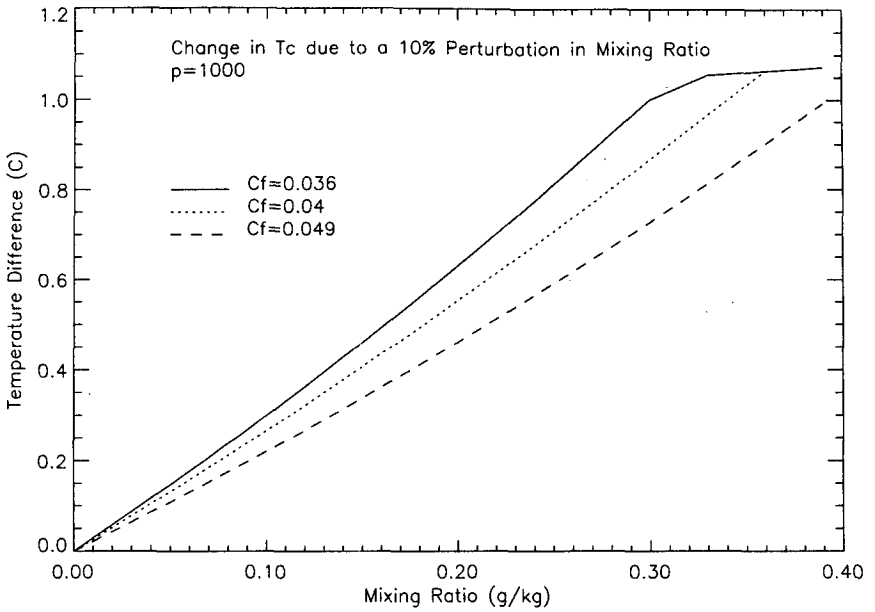

FIG. 6. Sensitivity of T_c to perturbations in w_a for several contrail factors.

dry and exhibits several mixing ratio inversion layers, the lowest of which peaks at around 6 km. Compare that with the temperature profile, which shows two inversions, with the lowest peaking at 1.5 km, corresponding to the minimum of the lowest mixing ratio inversion layer. As would be expected, this combination has the effect of depressing the critical temperature and creating an inversion for T_c as well. Also, as expected, the T_c profile for low-bypass engines is lower than for high-bypass engines. Both types of engines would generate contrails in this situation starting at around 7.5 km.

A very interesting feature of this sounding is that T_c for the low-bypass engine drops below the ambient temperature at around 14.5 km and remains below it until about 16.5 km. The effect of this is to produce

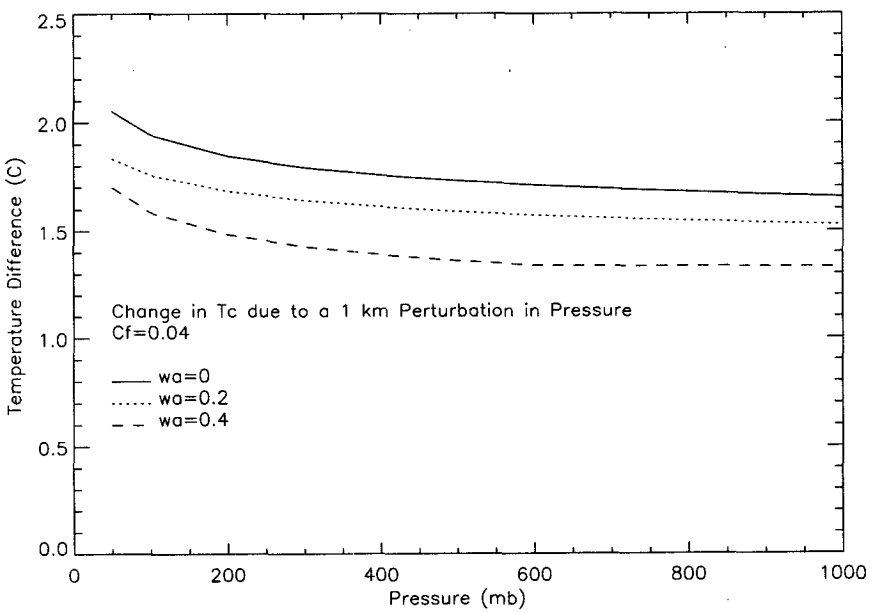

FIG. 7. Sensitivity of T_c to perturbations in p for several mixing ratios.

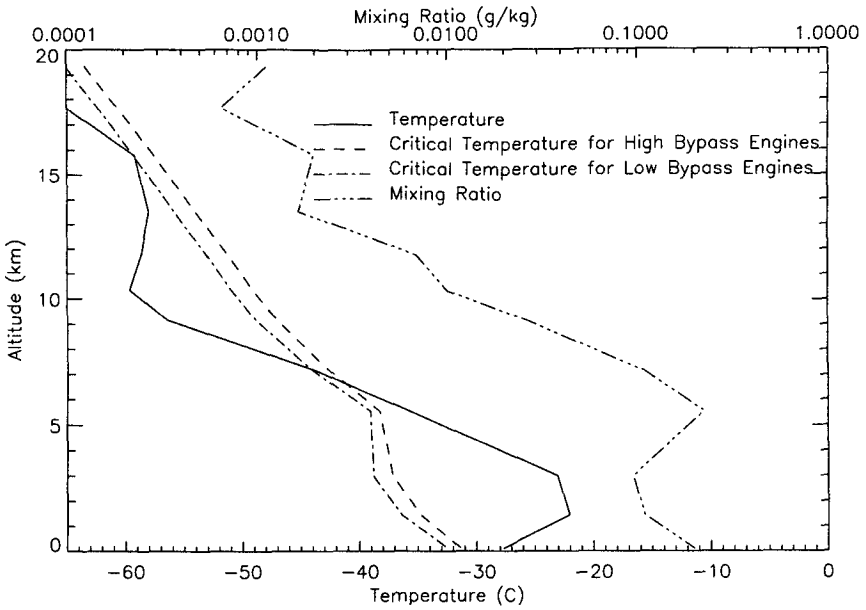

FIG. 8. Critical temperature for an arctic atmosphere for low- and high-bypass engines.

two distinct contrail formation layers for low-bypass engines, as distinct from the high-bypass-engine profile, which shows contrail formation conditions from 7.5 km up through 20 km without any break. Thus, an aircraft with low-bypass engines could find a high-altitude layer where contrails would be avoidable, while aircraft with high-bypass engines would have to remain below 7.5 km to avoid generating contrails.

Figures 9 and 10 show the difference in critical temperature between a relatively dry and a relatively wet midlatitude atmosphere taken from a RAOB for a low-bypass engine. The dry profile was taken at 40.65°N, 17.95°E, while the wet profile was taken at 41.65°N, 12.43°E. The temperature profile in both cases is quite similar, showing significant differences only above 10 km. The dry profile shows a distinctly dryer but colder tropopause relative to

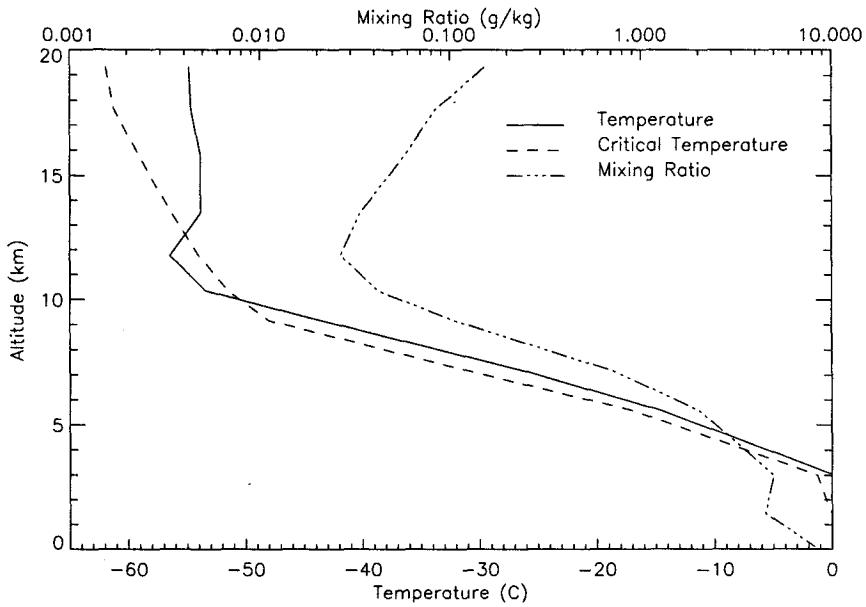

FIG. 9. Critical temperature for a relatively dry midlatitude atmosphere for a nonbypass engine.

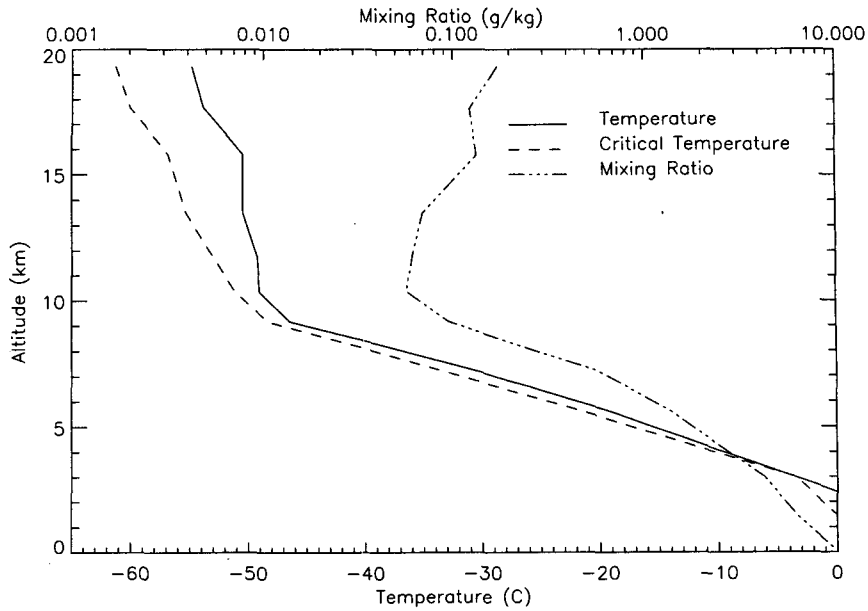

FIG. 10. Critical temperature for a relatively wet midlatitude atmosphere for a nonbypass engine.

the wet profile, with the result that a contrail formation layer exists in the "dry" sounding but is impossible in the "wet." This is somewhat counterintuitive but demonstrates that for a layer with sufficiently low temperature, no ambient water is necessary for contrail formation. Note also in the wet profile that between 3 and 4 km, T_c is equal to T, due to the fact that mixing ratio is high at that point relative to the dry profile. In fact the mixing ratio equals the saturation mixing ratio at 750 mb for this profile. The result is that for this very shallow layer a contrail might form but is unlikely.

10. Conclusions

A formulation of the contrail formation expression has been provided that is analytic and is expressed in terms of mixing ratio and pressure rather than relative humidity and pressure. Both represent improvements over previous formulations from the standpoint of actual forecasting technique and accuracy. The analytic formulation improves computational implementation. The formulation in terms of mixing ratio significantly reduces the sensitivity of the resulting critical temperature forecasts to errors or uncertainties in the moisture input by removing the effect of ambient temperature errors or uncertainties that are inherent in relative humidity.

Acknowledgments. The research for this paper was accomplished as part of support to the Defense Nuclear Agency under Contract F04701-93-C-0094. I am grateful to Major Robert Cox for consultations regarding forecasting aspects of the research described in this paper.

REFERENCES

Air Weather Service, 1981: Forecasting aircraft condensation trails. Air Weather Service Tech. Rep. AWS/TR-81/001, 46 pp. [DTIC AD-A111876.]

Appleman, H. S., 1953: The formation of exhaust condensation trails by jet aircraft. *Bull. Amer. Meteor. Soc.*, **34,** 14–20.

——, 1954: Memorandum on the effect of engine power setting on contrail formation and intensity. Air Weather Service Tech. Rep. AWS/TR-105-126, 4 pp. [DTIC AD-074310.]

——, 1957: Derivation of jet-aircraft contrail-formation curves. Air Weather Service Tech. Rep. AWS/TR-105-145, 46 pp. [DTIC AD-125760.]

Bjornson, B. M., 1992: SAC contrail formation study. USAF Environmental Technical Applications Center Project Rep. USAFETAC/PR-92/004, 48 pp. [DTIC AD-A254410.]

Bolton, D., 1980: The computation of equivalent potential temperature. *Mon. Wea. Rev.*, **108,** 1046–1053.

Knollenberg, R. G., 1972: Measurements of the growth of the ice budget in a persisting contrail. *J. Atmos. Sci.*, **29,** 1367–1374.

List, R. J., Ed., 1963: *Smithsonian Meteorological Tables.* 6th ed. Smithsonian Institution, 527 pp.

Miller, W. F., 1990: SAC contrail forecasting algorithm validation study. USAF Environmental Technical Applications Center Project Rep. USAFETAC/PR-90/003, 28 pp. [DTIC AD-B152198.]

Murcray, W. B., 1970: On the possibility of weather modification by aircraft contrails. *Mon. Wea. Rev.*, **98,** 745–748.

Peters, J. L., 1993: New techniques for contrail forecasting. Air Weather Service Tech. Rep. AWS/TR-93/001, 35 pp. [DTIC AD-A269686.]

Pilie, R. J., and J. E. Jiusto, 1958: A laboratory study of contrails. *J. Meteor.*, **15,** 149–154.

Saatzer, P., 1995: Pilot alert system flight test. Final Tech. Rep. for Period November 1988–May 1993, 241 pp. [Available from Northrup Grumman, B-2 Division, Northrup Grumman Corp., 8900 East Washington Blvd., Pico Rivera, CA 90660-3783.]

Sassen, K., 1979: Iridescence in an aircraft contrail. *J. Opt. Soc. Amer.*, **69,** 1080–1083.

Scorer, R. S., and L. J. Davenport, 1970: Contrails and aircraft downwash. *J. Fluid Mech.*, **43,** 451–464.